

Numerical investigations on innovative hollow section column-splice connections resorting to laser cutting technology

Rajarshi Das^{*,a}, Dan Dragan^a, Alper Kanyilmaz^b, Herve Degee^a

^aConstruction Engineering Research Group, Hasselt University, Diepenbeek 3590, Belgium
rajarshi.das@uhasselt.be, dan.dragan@uhasselt.be, herve.degee@uhasselt.be

^b Department of Architecture, Built Environment and Construction Engineering, Politecnico di Milano, Milan, Italy
alper.kanyilmaz@polimi.it

ABSTRACT

Hollow sections (HS) in general are gaining popularity in the construction sector due to their good resistance against high compression, tension and flexure in all directions, combined with their exceptional aesthetics. However, a conventional end plate-bolted connection between to HS members tend to limit their full potential by focusing most of the damages in the bolts, or making the chord vulnerable to localized yielding. Therefore, an efficient splice connection is required. To that purpose, innovative solutions are proposed in this paper and in the frame of an EU-RFCS project LASTTS, investigating a “passing-through” concept obtained through laser cutting technology (LCT). Three different column-splice connections are proposed: (1) CS-1: Square hollow section (SHS) columns connected using passing-through steel plates, bolts and steel cover plates outside the tube diameter; (2) CS-2: SHS columns connected using passing-through steel plates, bolts and steel cover plates inside the tube diameter; (3) CS-3: SHS columns connected using passing-through steel plates, bolts and steel end plates inside the tube diameter. All three types of connections have been investigated experimentally under tensile and bending forces. The structural behavior of the three different column-splice connections are compared among each other to highlight their advantages and disadvantages in terms of strength, stiffness and industrial application. The experimental results are then compared with analytical design calculations recommended by the European standards. Relevant conclusions are noted.

Keywords: Laser cut joints, Column splice connections, Passing-through joints, Hollow section joints

1 INTRODUCTION

An innovative “passing-through” concept was proposed in the recently concluded EU-RFCS research project – “LASTEICON” (1), where several tubular connections were developed using laser cutting technology (LCT) and investigated with the primary aim to characterize an efficient structural joint between open section beams and hollow section columns. The basic concept behind the passing-through joints are shown in Fig. 1. LASTEICON mainly focussed on different beam-to-circular hollow section (CHS) column connections consisting of “main” (primary) beams connected to the CHS column via one or multiple “through” elements (I-beam stub element or individual steel plates) passing through laser-cut slots on the CHS column. Thanks to their several advantages, both structural and economical, evidenced by experimental and numerical research investigations, the LASTEICON “passing-through” approach proved to be a viable alternative, and was therefore extended to a new European research project – “LASTTS” (2), where novel, specialised, and more complex joints were proposed to be investigated. One of such proposed aspects was to design innovative column splice joints using square hollow section (SHS) columns. This article presents

three different types of joint configurations designed and analysed for the laser-cut innovative splice connections applicable for SHS members. The different types of configurations are described below followed by the adopted modelling technique, boundary conditions as well as the numerical parametric studies. Relevant conclusions have been presented with further information regarding the planned experimental campaign.



Fig. 1. Laser cutting techniques, machine and approach to develop the LASTEICON and LASTTS joints (2)

2 LASTTS SPLICE CONFIGURATIONS

2.1 Types of Configurations

Three different column-splice configurations were proposed and investigated in the frame of the LASTTS project. The basic concept behind all three configurations remains the same. Steel plates are fully or partially inserted and welded in each of the two tubular pieces via laser cut slots. Then the two SHS members are connected together using different plates and bolt assemblies.

1) Column Splice 1 (CS-1): Two SHS columns are connected using passing-through steel plates (full depth of the plate is inserted in the tube), bolts and steel cover plates outside the tube diameter. Fig. 2a shows a schematic diagram of CS-1. Fig. 2b shows a schematic diagram and step-by-step assembly of CS-1. A front view is provided along with section cut view for better clarity. First, laser-cut slots are made in the SHS tubes and the two steel plates (with pre-determined bolt holes). The plates are inserted into each other and welded in the overlapping zone. Secondly, the plates are inserted and welded to the outer surface of each SHS tube. Finally, SHS 1 is connected to SHS 2 using bolts and cover plates joining the passing-through steel plates.

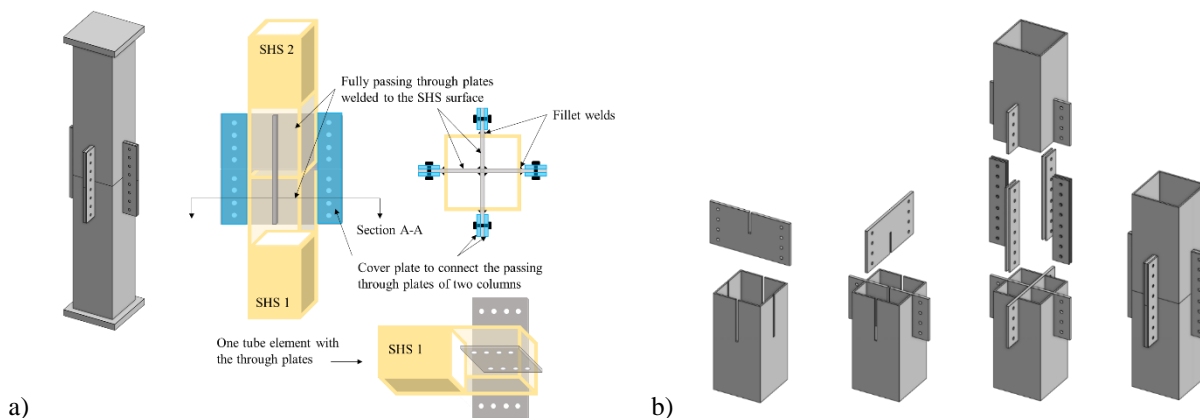


Fig. 2. CS-1 connection: a) Schematic diagram; b) step-by-step assembly

2) Column Splice 2 (CS-2): Two SHS columns are connected using passing-through steel plates (only partial depth of the plates is inserted in the tube), bolts and steel cover plates inside the tube diameter. Fig. 3a and Fig. 3b respectively shows a schematic diagram and step-by-step assembly of CS-2. First, laser-cut slots are made in the SHS tubes and the steel plates (with pre-determined bolt holes only on the top half of the plates). The plates are combined and welded in their overlapping zone. Secondly, the plates are inserted into the SHS and welded to the outer surface of the tube elements, using either fillet or full-penetration welds. Finally, SHS 1 (see Fig. 3a) is connected to SHS 2 using bolts and cover plates joining the passing-through steel plates. The primary difference between Splice CS-1 and CS-2 is the fact that, in case of CS-1, the splice connection is made outside the tubes whereas in case of splice CS-2, the connections are made inside the tube. The added value of splice CS-2 is its aesthetic appeal, as there is a negligible extension of the passing-through steel plates outside the SHS, and can therefore be visually more attractive.

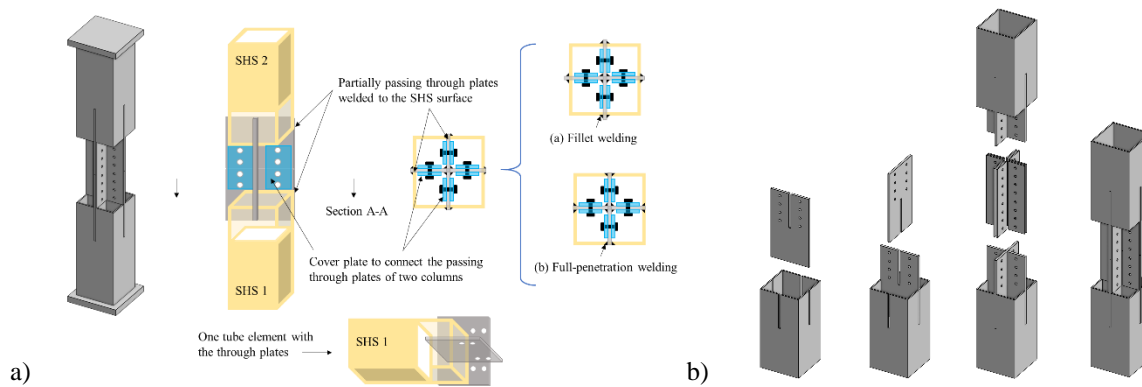


Fig. 3. CS-2 connection: a) Schematic diagram; b) step-by-step assembly

3) Column Splice 3 (CS-3): Two SHS columns are connected using passing-through steel plates (partial depth of the plate inserted in the tube), bolts and end connector plates inside the tube diameter. Fig. 4a and Fig. 4b respectively shows a schematic diagram and step-by-step assembly of CS-3. First, laser cut slots are made in the SHS and the two orthogonally placed steel plates (without any pre-determined bolt holes on the plates). The plates are then inserted into each other and welded together. Secondly, the plates are inserted into the SHS elements through the laser-cut slots and are welded to the outer surface of the tubes using either fillet or full penetration welds. Thirdly, the free side of the passing-through plates are welded to end connector plates (with pre-determined bolt holes). Finally, SHS 1 is connected to SHS 2 using bolts. The primary difference between the Splice CS-2 and CS-3 configuration is basically the bolt assembly which leads to a different force-transfer mechanism in the bolts (i.e. tensile forces instead of shear forces).

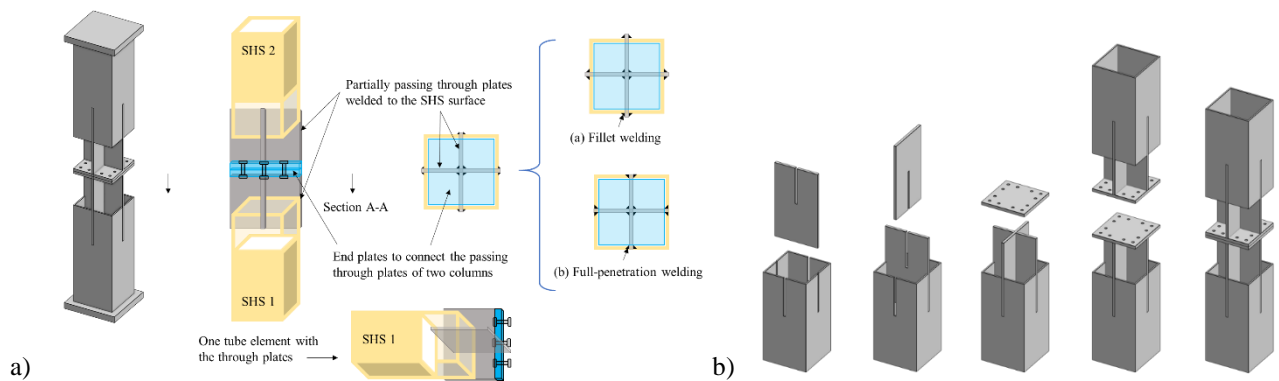


Fig. 4. CS-3 connection: a) Schematic diagram; b) step-by-step assembly

2.2 Modelling approach and boundary conditions

The splice configurations were modelled using 3D solid elements and analyzed through nonlinear static analyses in the FE commercial software DIANA FEA (3). The laser-cut slots corresponding to the passing-through elements were considered on the SHS to account for the necessary reduction in the tube stiffness. However, certain assumptions were made in order to avoid a complicated model at such a preliminary stage. A zero tolerance was assumed between the passing through elements and the SHS, therefore assuming a perfectly welded connection. The weld failure was not modelled explicitly to avoid convergence issues and heavy computation time. The bolts were consciously analytically designed with an overstrength for the experimental campaign. So, they were modelled with elastic material properties, in order to avoid any secondary failure in the splice connection and rather focus on the unknown vulnerabilities of the splice. The steel plates used at both ends of the SHS elements to apply the boundary conditions and loads were also modelled with linear elastic properties.

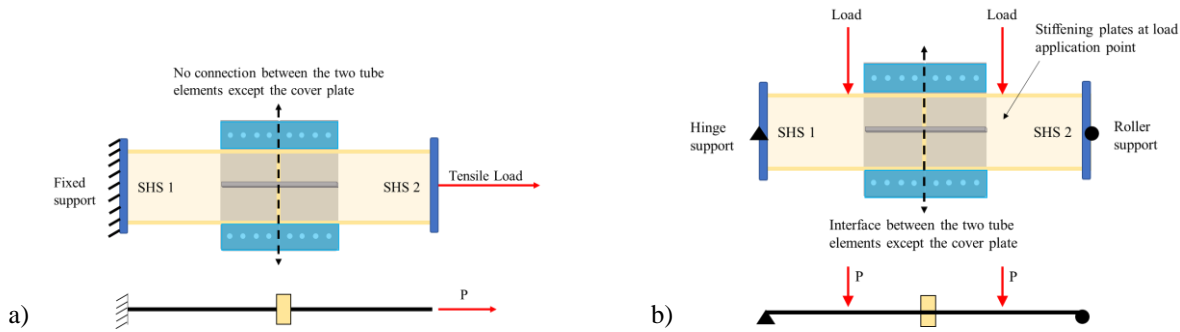


Fig. 5. Boundary conditions, load application and modelling choices for a) tensile load case; b) bending load case

Two load cases were considered – tension (Fig. 5a) and 4-point bending (Fig. 5b). Modelling choices were made depending on the specific load cases: (1) For the tensile load case, one end of the joint was fixed while a tensile load was applied at the other end. The direct contact was considered between the two SHS elements (for the tubes and the passing-through plates, referred by the dotted line in Fig. 5a) – which therefore ensured that SHS 1 and SHS 2 were connected only via the cover plates bolted to the through plates. A similar approach was followed for splice CS-2 (no connection between the passing-through plates of the different tube elements) and splice CS-3 (no connection between the end connector plates); (2) For the 4-point bending analysis, a simply supported boundary condition was considered. One end of the joint was hinged while the other end was given a roller. Both supports were provided along a line rather than a single node to avoid stress concentrations. Vertical loads of equal magnitude were applied at the half-way length of each tube (SHS 1 and SHS 2) as shown in Fig. 5b – ensuring that the distance between the point of load application and the point of support remains the same for CS-1, CS-2 and CS-3. Stiffening plates were used inside the tubes at the location of load application to avoid local crushing. An interface was modelled on the surfaces (of the tube and the passing-through plates shown by the dotted line in Fig. 5b) between the two SHS. This interface was defined by a high stiffness under compression and negligible stiffness under tension - which therefore guaranteed that the two tube elements would open up under tension and would come into contact other under compression. A similar approach was followed for splice CS-2 (interface between the passing-through plates of the different tube elements) and splice CS-3 (interface between the square end connector plates). Geometric nonlinearity was considered in the numerical simulations. Material nonlinearity was introduced in the models for the tubular columns, passing-through plates, cover plates (for splice CS-1 and CS-2), end connector plates at the central connection zone (for splice CS-3) as an elastic perfectly plastic material behaviour of S355 (yield stress, $f_y = 355$ MPa). The FE modelling approach was validated based on previous experimental investigations done in the frame of LASTEICON (1).

3 RESULTS AND DISCUSSIONS

3.1 Tensile behaviour of the connections

8 different SHS splice connections (geometric properties are shown in Table 1) were investigated for the 3 different configurations under a tensile load through nonlinear static analyses. The load was incremented step by step from 0 till failure was reached. In this numerical sensitivity study, “failure” is defined as reaching a limiting value of the equivalent plastic strain value (= 5%), obtained while calibrating the LASTEICON experimental results. Some properties were kept constant throughout the models: (1) in all cases, the length of one SHS tube was considered = 1000 mm. Depending upon the splice configurations, the total length of the splice connection varied: for splice CS-1 the total length is = 2120 mm, for splice CS-2 the total length is = 2820 mm and for splice CS-3 the total length is = 2580 mm. However, the length variation does not influence the tensile or bending behaviour of the splices; (2) the width of the through plate was kept consistent with respect to the tube = width of the SHS + 300 mm; (3) the width of the end connection plates used in splice CS-3 was kept equal to that of the tube itself.

Table 1. Geometric properties of the SHS column splice case studies

Case No.	Geometric properties (in mm)								
	SHS column		Cover plate		Through plate		Bolts		Con. Plate
	side	thick	width	thick	depth	thick	dia.	No./grade	side × thick
1	350.0	10.0	140.0	20	354	20	24	32@M10.9	NA
2	250.0	10.0	140.0	20	354	20	24	32@M10.9	NA
3	400.0	10.0	140.0	20	354	20	24	32@M10.9	NA
4	350.0	12.5	140.0	20	354	20	24	32@M10.9	NA
5	350.0	12.5	140.0	20	354	20	20	32@M10.9	NA
6	350.0	12.5	140.0	20	354	10	20	32@M10.9	NA
7	350.0	12.5	155.0	20	700	20	24	32@M10.9	NA
8	350.0	12.5	NA	NA	400	20	24	32@M10.9	350 × 30

For splice CS-1, 6 cases (Case 1 – Case 6) were investigated with varying tube wall thickness, side width, thickness of the through plates, etc. Splice CS-2 was investigated through Case 7 and Splice CS-3 was investigated through Case 8. Analytical calculations were conducted in order to predict the ultimate strength and failure. According to the analytical calculations, 8 failure modes (FM) were identified in total (for all three types of splice configurations): (i) FM1: shear failure of the bolts, (ii) FM2: bearing failure of steel plates (cover and passing through), (iii) FM3: tensile failure of the cover plate, (iv) FM4: shear failure of the passing through plates, (v) FM5: tensile failure of the tube, (vi) FM6: tensile failure of the passing through plates, (vii) FM7: tensile failure of bolts, (viii) FM8: plasticity at the end connection plates. The first 5 failure modes (FM1 – FM5) were identified for splices CS-1 and CS-2, whereas FM6 was obtained for splice CS-2 only and FM4, FM5, FM7 and FM8 were realized for splice CS-3. In order to avoid any failure of the bolts (which is quite straightforward and have been studied in numerous researches in the past), they were kept elastic in the numerical models. Additionally, they were perfectly connected to the steel plates (without defining a special contact surface) to avoid complicated models for the preliminary studies. Due to these two assumptions, the shear/tensile failure of the bolts (FM1/FM7) and bearing failure of the plates (FM2) could not be predicted by the numerical models. However, such failure modes will be integrated during the calibration studies based on the experimental investigations (soon to be realized). Detailed analytical calculations can be found in (2). Table 2 summarizes the analytically estimated failure modes including shear failure of bolts and the bearing failure of the plates to have an idea about the actual failure mode and also excluding them to have a direct comparison with the numerical results obtained through the FEA. The load-displacement curves obtained from the case studies of CS-1 are shown in Fig. 6, where the horizontal lines represent the analytically calculated

values for the relevant failure mechanisms obtained from the numerical models, i.e. FM3, FM4 and FM5. Fig. 7 illustrates the stress contours obtained from Case 4, Case 6 and Case 2.

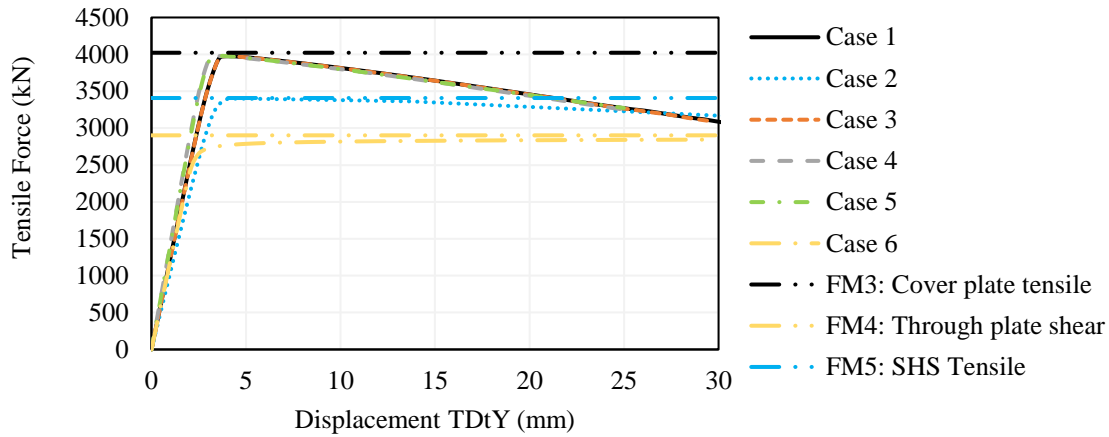


Fig. 6. Load-displacement curves obtained from all case studies (SHS) – tension load

Table 2. Analytically estimated strength and failure modes of CS-1 case studies with and without FM1 and FM2

CS-1	Failure modes					min {FM1-FM5}		min {FM3-FM5}	
	FM1 (kN)	FM2 (kN)	FM3 (kN)	FM4 (kN)	FM5 (kN)	Strength (kN)	Failure (kN)	Strength (kN)	Failure (kN)
Case 1	4518.4	3775.3	4021.9	5804.4	4828.0	3775.3	FM2	4021.9	FM3
Case 2	4518.4	3775.3	4021.9	5804.4	3408.0	3408.0	FM5	3408.0	FM5
Case 3	4518.4	3775.3	4021.9	5804.4	5538.0	3775.3	FM2	4021.9	FM3
Case 4	4518.4	3775.3	4021.9	5804.4	5990.6	3775.3	FM2	4021.9	FM3
Case 5	3136.0	4407.0	4163.0	5804.4	5990.6	3136.0	FM1	4163.0	FM3
Case 6	3136.0	2203.5	4163.0	2902.2	5990.6	2203.5	FM2	2902.2	FM4

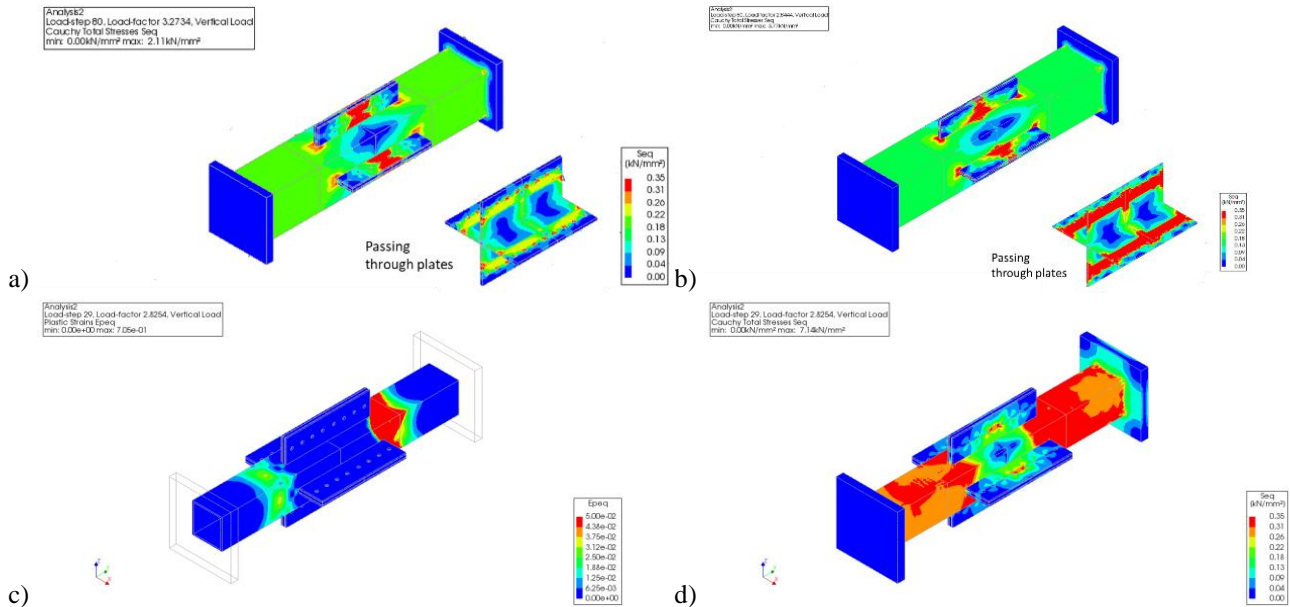


Fig. 7. von Mises stresses for a) Case 4; b) Case 6; c) equivalent plastic strains and d) von Mises stresses for Case 2

According to the load-displacement curves as well as the analytical calculations, it was clearly seen that increasing the side width or the thickness of the SHS tube does not affect the connection's tensile resistance if the failure mode is governed by the other elements of the splice (cover plates,

through plates etc.). For instance, a tensile failure of the cover plate was obtained in Case 1, Case 3, Case 4 and Case 5 from both the analytical predictions as well as the numerical simulations (see Fig. 7a for Case 4). A wider or thicker SHS tube did not provide much influence in these cases. A similar aspect can be noticed also for Case 6, where the thinner plates (10 mm) were passed through to realize the splice connections. They failed due to shear stress in the through plates (see Fig. 7b). However, when the failure is governed by the tube element itself due to a lesser cross-section area (width and thickness), it can also become vulnerable towards tensile failure as observed in Case 2 (see Fig. 7c and Fig. 7d). In this case the stresses were observed to first develop at the corners of the connection zone between the tube and the passing-through plates, which then spread through the tube. Limiting values of the plastic equivalent strains and von Mises stresses at maximum load were reached in the tube prior to the cover plates or the passing-through plates. The numerical results were observed to agree well with the analytical estimations.

Only one case study was investigated each for splice configurations CS-2 and CS-3 as mentioned in Table 1. Fig. 8 presents the comparison between the load-displacement behaviour of splices CS-1, CS-2 and CS-3 having similar geometrical properties (for the SHS column and the passing through plates, i.e. Case 4, 7 and 8). Fig. 9 and Fig. 10 respectively shows the plastic equivalent strains and von Mises stresses for Case 7 and Case 8.

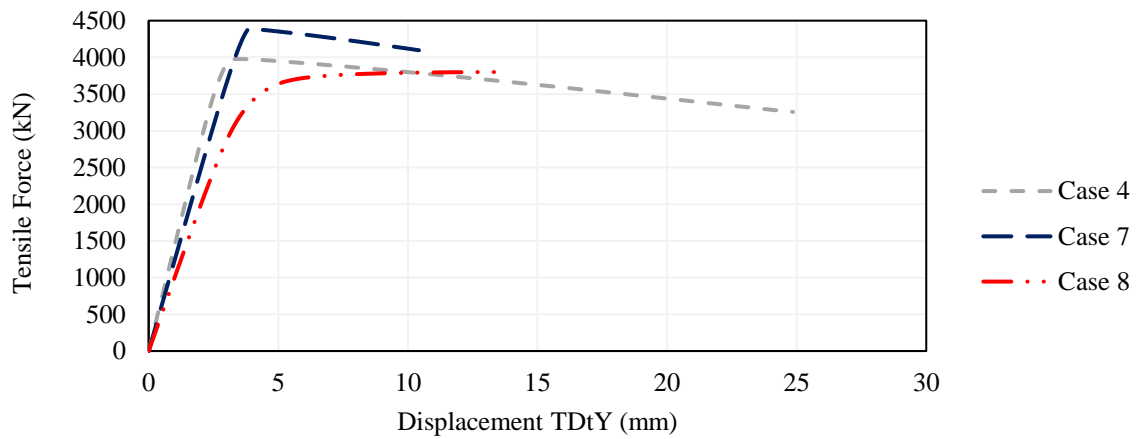


Fig. 8. Comparing load-displacement curves among CS-1, CS-2 and CS-3– tension load

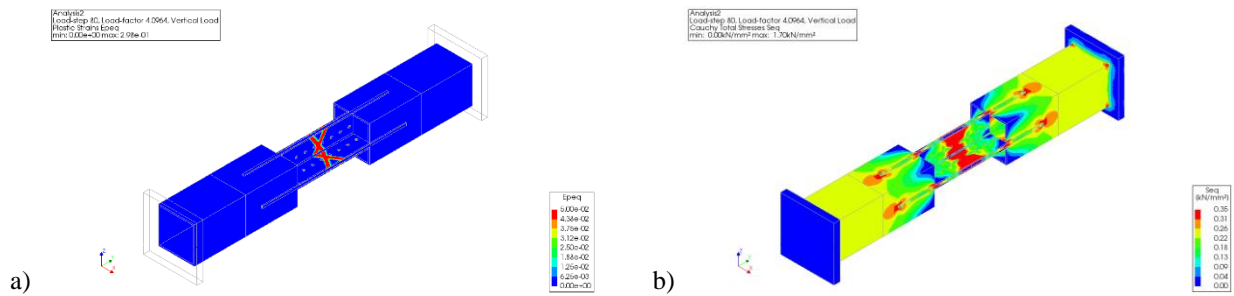


Fig. 9. a) Equivalent plastic strains; b) von Mises stresses for Case 7 (splice CS-2) at maximum load

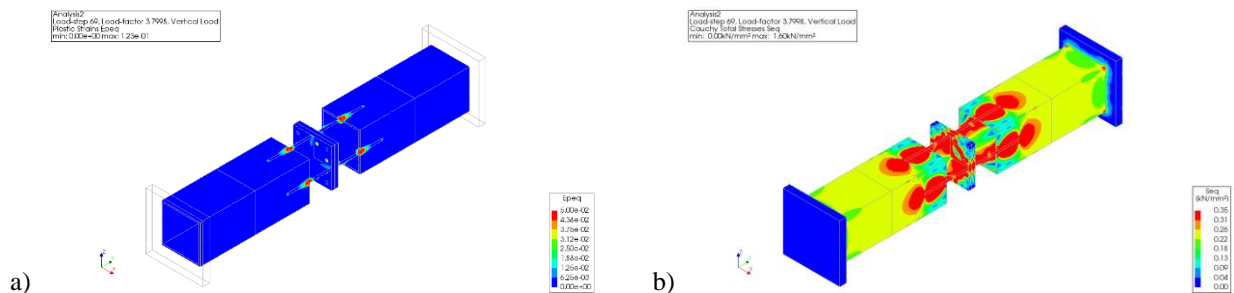


Fig. 10. a) Equivalent plastic strains; b) von Mises stresses for Case 8 (splice CS-3) at maximum load

Comparing the load-displacement curves between the splice CS-1 and splice CS-2 case studies with similar geometrical properties (Case 4 vs Case 7), such as the width and thickness of the SHS, thickness of the cover plates and through plates etc., it can be noticed that the splice CS-2 connection offers a better resistance than the splice CS-1 connection. This occurs due to a slightly wider cover plate in splice CS-2 (Case 7 - 155 mm) compared to splice CS-1 (Case 4 - 140 mm). However, the analytical and numerical failure mode was obtained to be similar for Case 4 and Case 7 i.e. a tensile failure of the cover plate (see Fig. 7a and Fig. 9). The case study for splice CS-3 (Case 8) was also compared with splices CS-1 (Case 4) and CS-2 (Case 7) having similar geometric properties for the tube, through plates, etc. The CS-3 configuration provided an approximately equal resistance as the CS-1 configuration. As shown by the von Mises stresses in Fig. 10, the numerical failure in this case was realized at the connection zone of the passing-through steel plates and the SHS tubes due to high tensile stresses. Significant stresses were also noticed in the passing-through plates and the steel connection plates between the two SHS elements.

3.2 Flexural behaviour of the connections

Identical case studies, as listed in Table 1, were investigated through a 4-point bending load condition through nonlinear static analyses. Load-displacement curves are plotted with respect to one of the vertical loads vs the vertical displacement obtained at the center of the splice connection. The load-displacement curves obtained from all case studies are shown in Fig. 11.

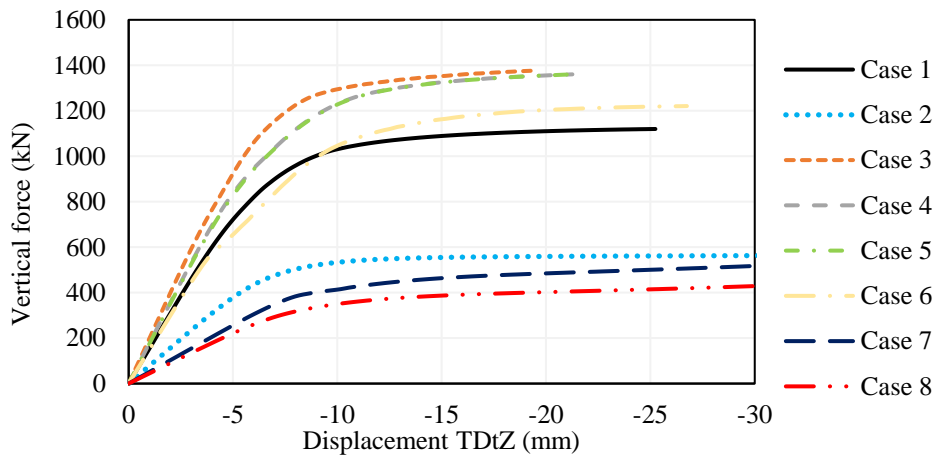


Fig. 11. Load-displacement curves obtained from all case studies – bending load

According to the load-displacement behaviour of the different case studies, it was observed that – (1) increasing the cross section (side width and thickness) of the tube increases the bending resistance of the splice connection; and (2) increasing the thickness of the through plates increases the resistance of the splice connection. As the above-mentioned parameters change the section modulus of the splice connection at the center, they directly affect the flexural resistance of the splice connections. Fig. 12 shows the von Mises stresses for Case 1, Case 2, Case 4 and Case 6. In case of splice CS-1, the stresses and strains initiated at the corners of the connection zones between the passing-through plates and the SHS column (tube wall tearing/crushing) and then spread through the tube. As shown in Fig. 12a, failure stresses were obtained in both the SHS tube (350 mm width and 10 mm thickness) and the cover plates of the splice connection for Case 1. However, for Case 2 (250 mm width and 10 mm thickness), the stresses concentrated in the tube alone due to its reduced cross-section (see Fig 12b). Results for Case 3 and Case 4 were similar to that of Case 1. The von Misses stresses for Case 4 is shown in Fig. 12c. For these three case studies (Case 1, Case 3 and Case 4), the passing through plates (20 mm thick) did not showcase any considerable damage. However, in Case 6 (10 mm thick passing through plates), substantial yielding was observed in the passing through plates along its connection length with the tube (see Fig. 12d).

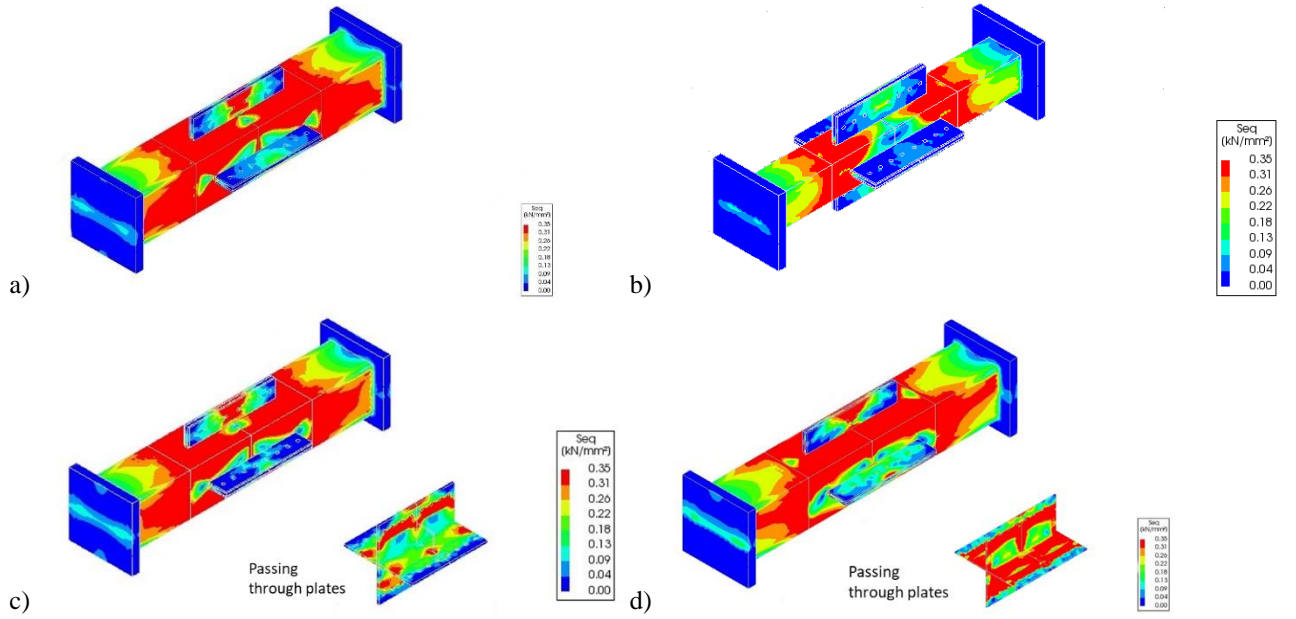


Fig. 12. von Mises stresses for splice CS-1: a) Case 1; b) Case 2; c) Case 4; d) Case 6 at maximum load

Significantly different results were found from the splice CS-2 and CS-3 configurations. If we compare the force-displacement behaviour (see Fig. 11) of the splice CS-1, CS-2 and CS-3 case studies with similar geometrical properties for the tube, through plates etc. (i.e. Case 4, Case 7 and Case 8), a substantial reduction in resistance was obtained for splice CS-2 and CS-3 compared to splice CS-1. Fig. 13 and Fig. 14 respectively shows the numerical results for splice CS-2 (case 7) and CS-3 (case 8) configurations.

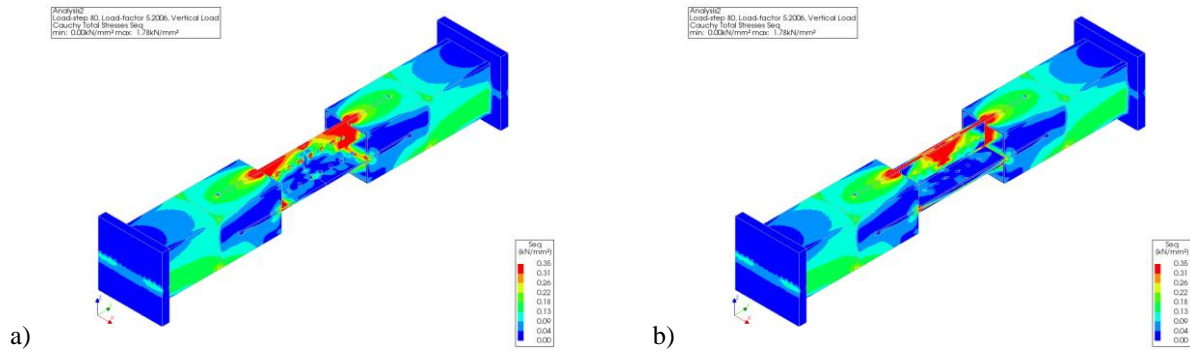


Fig. 13. von Mises stresses in Case 7 (splice CS-2): a) in the passing through; b) cover plates at maximum load

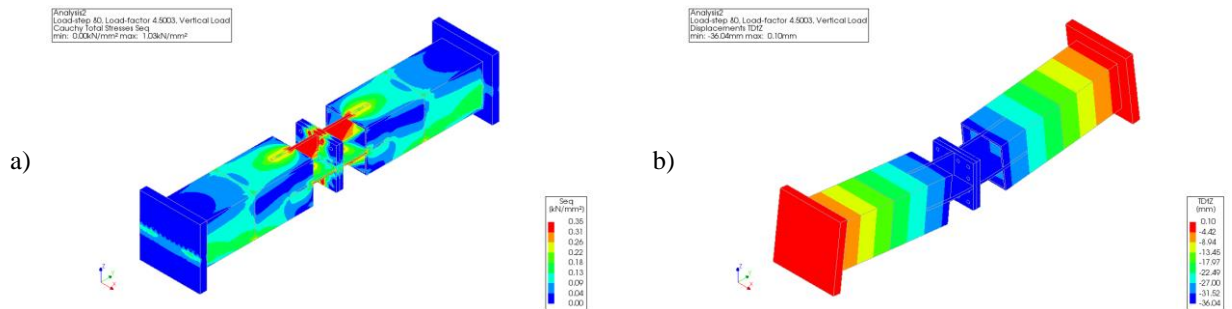


Fig. 14. a) von Mises stresses; b) deformed shape of Case 8 (splice CS-3) at maximum load

As can be seen from the von Mises stresses illustrated in Fig. 13 and Fig. 40, the damages in both splice CS-2 and CS-3 concentrate in the passing-through plates, cover plates or end connector plates in the central connection zone rather than the SHS columns. As already anticipated, for both these configurations, the SHS tube offered a negligible contribution to the flexural resistance of the splice connection – which therefore explains the substantial reduction in their resistances.

4 CONCLUSIONS

Three different types of laser-cut “passing-through” SHS column splice connections have been proposed in this article. The connection configurations were designed based on the existing European standards and were investigated using 3D finite element models through nonlinear static analyses. The finite element modelling approach was validated based on experimental results, obtained in the frame of a recently concluded EU-RFCS research project LASTEICON – dealing with similar passing-through I-beam-to-CHS column joints. 8 different case studies were analyzed analytically and numerically considering two load cases – (i) a tensile load and (ii) a 4-point bending load. Different failure modes were identified and discussed for all three types of splice configurations. Significant conclusions could be drawn from the results. The numerical results were observed to be in good agreement with the analytical estimations of the ultimate strength and the failure mode of the splice connections. Depending on the failure modes, the numerical models showed that the main parameters influencing the tension and bending resistance are the cover plates’ thickness, the through plates’ thickness and the column section (diameter and thickness of the CHS). Nevertheless, certain modelling assumptions were made in order to avoid complicated models at such a preliminary design stage. The bolts were kept elastic and were perfectly connected to the steel plates (without defining a special contact surface) in the numerical models which therefore limited the model’s capacity to predict certain failure modes: the tensile and shear failure of the bolts, the bearing failure of the plates. Such failure criteria will be duly integrated in the numerical models during the calibration studies, once the experiments are done – planned to be conducted in March 2024 on 10 splice connections. Furthermore, the different types of welds, i.e. full strength or partial strength fillet welds and full penetration welds will be investigated to understand their influence and viability in the proposed splice connections.

5 ACKNOWLEDGMENT

This project has received funding from the European Union, Research Fund for Coal and Steel under grant agreement No 101034038. Views and opinions expressed are however those of the author(s) only and do not necessarily reflect those of the European Union or Research Fund for Coal and Steel. Neither the European Union nor the Research Fund for Coal and Steel can be held responsible for them.

REFERENCES

1. **Castiglioni, C.A., et al.** *LASTEICON - Laser Technology for Innovative Joints in Steel Construction*. Brussels, Belgium : EU-RFCS, 2016-2019. Final report. RFCS-GA-709807.
2. **Kanyilmaz, A., et al.** *LASTTS - Laser cutting technology for tubular structures*. s.l. : EU-RFCS, 2022. Mid-term project report. 101034038.
3. **Version 10.7, DIANA FEA.** <https://dianafea.com/>. [Online] Computational Mechanics department of TNO Building and Construction Research Institute in Delft, The Netherlands., 2023. <https://dianafea.com/>.